Amino Ether-Phenolato Precatalysts of Divalent Rare Earths and Alkaline Earths for the Single and Double Hydrophosphination of Activated Alkenes

Ivan V. Basalov, Bo Liu, Thierry Roisnel, Anton V. Cherkasov, Georgy K. Fukin, Jean-François Carpentier, Yann Sarazin, Alexander A. Trifonov

Aminoether-phenolato Precatalysts of Divalent Rare Earths and Alkaline Earths for the Mono and Double Hydrophosphination of Activated Alkenes

Ivan V. Basalov,† Bo Liu,§ Thierry Roisnel,§ Anton V. Cherkasov,† Georgy K. Fukin,† Jean-François Carpentier,*,§ Yann Sarazin*,§ and Alexander A. Trifonov*,†

† G. A. Razuvaev Institute of Organometallic Chemistry of Russian Academy of Sciences, Tropinina 49, GSP-445, 603950 Nizhny Novgorod (Russia).

§ Institut des Sciences Chimiques de Rennes, UMR 6226 CNRS – Université de Rennes 1, Organometallics: Materials and Catalysis group, Campus de Beaulieu, 35042 Rennes (France)

Entry for the Table of Contents

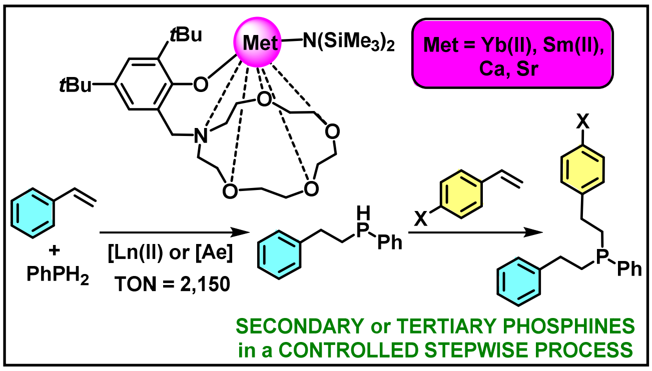

■ ABSTRACT

A range of stable ytterbium(II) aminoether-phenolato amido complexes of the type $\{LO^{NxOy}\}Yb\{N(SiMe_3)_2\}$, together with a congeneric samarium(II) and two calcium and strontium amido and alkyl derivatives, have been synthesized. They constitute very active, fully regioselective (*anti*-Markovnikov) and chemoselective precatalysts for the intermolecular hydrophosphination of styrene derivatives with $PhPH_2$, achieving TON up to 2,150, TOF up to 30 h^{-1} and chemoselectivity in the region 95-99%. The ytterbium(II) precatalysts, amongst which most prominently $\{LO^{NO4}\}Yb\{N(SiMe_3)_2\}$ (**3**) where the ligand possesses a 15-c-5-aza-crown-ether side-arm, outperform their related calcium analogues and the activity of the catalyst increases substantially with the denticity of the ligand. The rate law *rate* = *k*.[*p*-^{t}Bu-styrene].[**3**] was established following kinetic monitoring of the hydrophosphination of *p*-^{t}Bu-styrene and $PhPH_2$ catalyzed by **3**. The kinetic studies also revealed that the reactions are entropically driven, and that reaction rates increase when electron-withdrawing groups are introduced in *para* position of the styrenic substrate. It is proposed that these catalyzed hydrophosphination reactions proceed by rate-limiting olefin insertion into the [Yb]–phosphide bond. The chemoselective one-pot, two-step double hydrophosphination of $PhPH_2$ with two equiv of styrene yields tertiary phosphines. It obeys an unusual kinetic profile where formation of the tertiary phosphine starts only when complete consumption of $PhPH_2$ is first ensured. This sequence was used to obtain asymmetric tertiary phosphines with excellent selectivity.

■ INTRODUCTION

The creation of C–P bonds by catalyzed intermolecular hydrophosphination of activated alkenes (acrylonitrile, acrylates, dienes and styrene) has been the focus of increasing attention in recent years, because it affords a clean, atom-efficient access to valuable phosphine derivatives.[1] This catalysis originally relied prominently on catalysts designed around nickel,[2] palladium,[3] platinum[4] with Michael-type substrates or, at the opposite end of the *d* block, lanthanides.[5] The development of these earlier catalysts has been covered in many a comprehensive review.[6] More recently, systems based on copper,[7] iron,[1f] tin[8] or more oxophilic metals, *e.g.* titanium/zirconium,[9] alkaline earths[10] and divalent lanthanides,[10c-d,11] have also proved very competent. A case of FLP-mediated hydrophosphination of alkenes has also been reported.[12] A substantial breakthrough was Waterman and coworkers' account of a zirconium precatalyst for the hydrophosphination of unactivated alkenes such as 1-hexene, a remarkable result for such notoriously reluctant substrates.[9b] Substrate scope in this catalysis remains in fact rather limited, and chiefly involves the benchmark hydrophosphination of activated olefins with the ubiquitous diphenylphosphine. Reactions with primary phosphines such as phenylphosphine remain rather seldom,[8a,9b-c,11] although the resulting secondary phosphine products are of obvious interest to organic and coordination chemists alike.

Even if *trivalent* lanthanide (Ln) complexes catalyze the polymerization,[13] hydrogenation,[14] hydrosilylation,[15] hydroamination,[16] hydrophosphination,[17] hydroalkoxylation,[18] hydrothiolation[18] and hydroboration[19] of olefins, little has been said of the ability of *divalent* lanthanide complexes to promote these reactions. This is somewhat peculiar, as the larger ionic radii and the redox-active nature of Ln(II) ions (effective ionic radii for C.N. = 6: Yb^{2+}, 1.02 Å; Eu^{2+}, 1.17 Å; Sm^{2+}, 1.22 Å; standard oxidation potentials: Yb^{3+}/Yb^{2+}, −1.05 V; Eu^{3+}/Eu^{2+}, −0.35 V; Sm^{3+}/Sm^{2+}, −1.55 V) warrants exciting properties in catalysis; the situation in part stems from inherent synthetic difficulties associated with these reactive elements. Like for the Ln(II) ytterbium, europium and samarium congeners, complexes of the large, oxophilic alkaline earths (Ae) calcium, strontium and barium (r_{ionic} = 1.00, 1.18 and 1.35 Å, respectively) have d^0 outer-shell electronic configuration. Ln(II) and Ae compounds bearing the same bulky ligand often exhibit analogous structural features. Although Ae complexes display greater Lewis acidity and ionic character,[20] the filling of low-lying f orbitals (Sm(II), $4f^6$; Eu(II), $4f^7$; Yb(II), $4f^{14}$) of limited radial extension is presumed not to alter fundamentally the reactivity of Ln(II) complexes with respect to that of their Ae congeners. In fact, their reactivities often match closely,[21] but they can in some cases show marked differences, *e.g.* in polymerization catalysis.[22] Our research groups have been involved for a few years in the design of isoelectronic Ln(II) and Ae precatalysts to mediate organic transformations, in particular with a view to devising efficient tools for the production of C–P bonds. If bulky ligands were shown to be redundant in the hydrophosphonylation of carbonyls,[23] nitrogen-based amidinates and iminoanilides proved formidable assets in the hydrophosphination of alkenes.[10d,11a,11c] In a preliminary communication, we have described the utilization of Yb(II) and Sm(II) complexes supported by multidentate, monoanionic aminoether-phenolates to promote the chemoselective and regioselective (anti-Markovnikov) addition of phenylphosphine to styrene.[11b] The full extent of this study, which includes structural characterization, kinetic investigations and comparison of Ln(II) and Ae precatalysts, is now reported.

■ RESULTS AND DISCUSSION

Synthesis and characterization

The aminoether-phenolato ytterbium(II) complexes $\{LO^{(NO)2}\}Yb\{N(SiMe_3)_2\}$ (**1**, dark red), $\{LO^{NO2}\}Yb\{N(SiMe_3)_2\}$ (**2**, orange) and $\{LO^{NO4}\}Yb\{N(SiMe_3)_2\}$ (**3**, bright yellow) were obtained free of coordinated THF in 80–90% isolated yields upon amine elimination in the stoichiometric reactions of $Yb\{N(SiMe_3)_2\}_2$•$(THF)_2$ with the protio-ligands $\{LO^{(NO)2}\}H$, $\{LO^{NO2}\}H$ or $\{LO^{NO4}\}H$ in toluene (Scheme 1). The Sm(II) derivative $\{LO^{NO4}\}Sm\{N(SiMe_3)_2\}$ (**4**, black) was obtained in 40% yield by a same protocol. The synthesis of these complexes and the molecular solid-state structures of **2** and **4** were described in our initial communication.[11b] The known calcium amido complexes $\{LO^{(NO)2}\}Ca\{N(SiMe_3)_2\}$ (**5**) and $\{LO^{NO2}\}Ca\{N(SiMe_3)_2\}$ (**6**), the syntheses and crystallographic structures of which were reported independently,[24] were included in the catalytic study for comparative purposes. The new colorless alkyl complexes $\{LO^{NO2}\}Ca\{CH(SiMe_3)_2\}$•THF (**7**) and $\{LO^{NO2}\}Sr\{CH(SiMe_3)_2\}$ (**8**) were obtained in 55−70% yield upon equimolar treatment of the corresponding precursors $Ae\{CH(SiMe_3)_2\}_2$•$(THF)_2$ (Ae = Ca, Sr) with $\{LO^{NO2}\}H$ in pentane. Peculiarly, the calcium complex **7** could not be obtained free of THF, even upon gentle heating under dynamic vacuum, although its strontium derivative **8** was devoid of any coordinated solvent, despite the much larger metallic center. Other examples of stable heteroleptic Ae-alkyl complexes are rather seldom, and are restricted to the use of bulky alkyl groups such as bis(trimethylsilyl)methyl[10b-c,25] and substituted benzyl moieties.[26] The ^{1}H NMR data for **7** (in benzene-d_6) and **8** (in THF-d_8) are characterized by very high-field resonances for the methyl [Ae]−C*H* hydrogen atoms, at δ_{1H} −1.87 and −2.20 ppm, respectively. The presence of coordinated THF in **7** is confirmed by multiplets at 3.60 and 1.40 ppm integrating for 4H each.

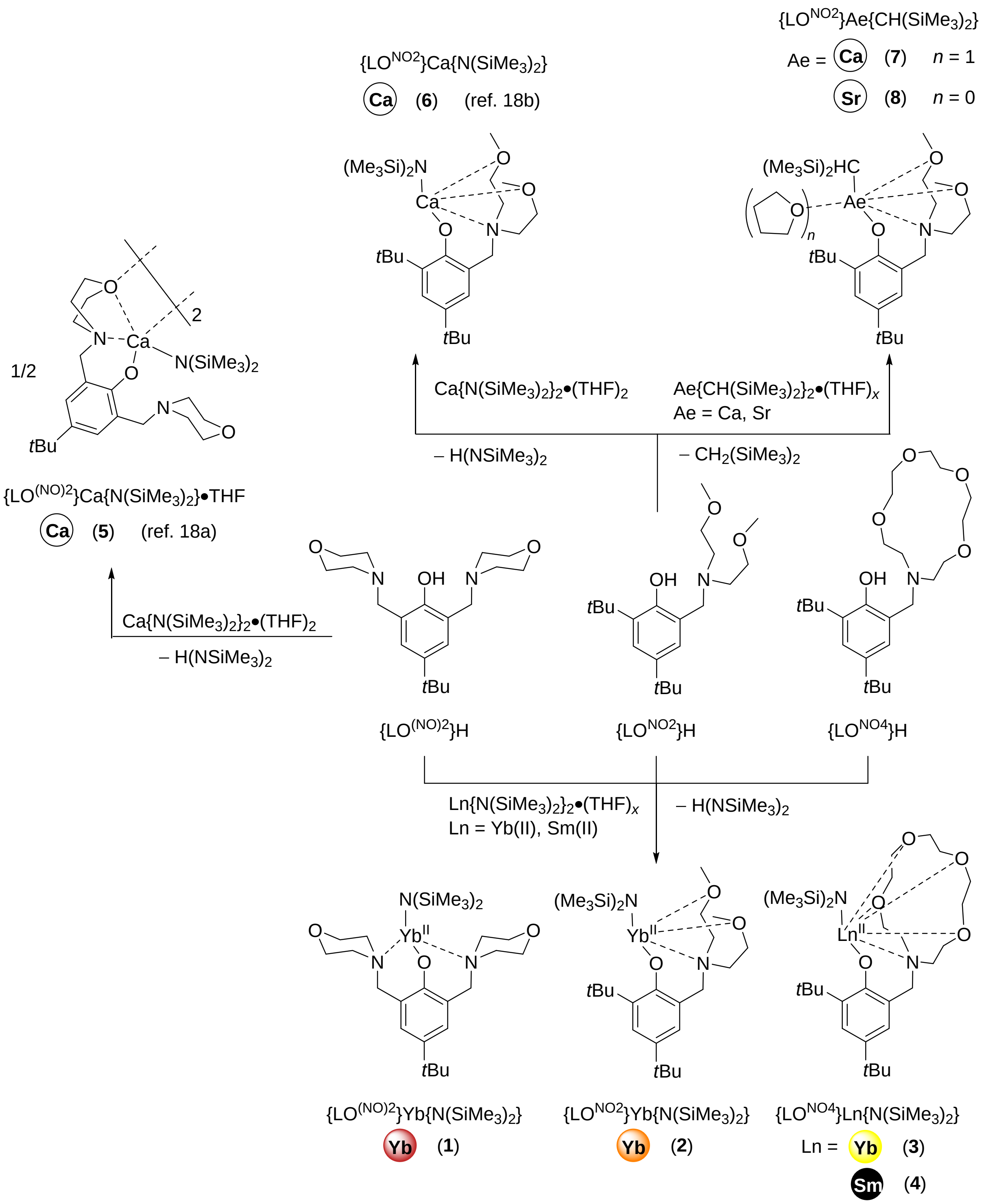

Scheme 1. Synthesis of the divalent lanthanide (**1-4**) and alkalino-earth complexes (**5-8**) supported by aminoether-phenolato ligands. For complexes **5-6**, see reference 24. The bonding patterns are structurally established for **2-7**, but they are hypothetical for **1** and **8**.

The heteroleptic calcium complex **7** is stable in aromatic hydrocarbons, without signs of decomposition or ligand scrambling after two days at room temperature. However, the strontium complex **8** is more kinetically labile, and its ^{1}H NMR spectrum at room temperature always shows contamination by *ca*. 3−5 mol-% of the homoleptic species $\{LO^6\}_2Sr$ and an unidentified strontium-alkyl species; the proportion of homoleptic complexes increased with temperature. The action of $Sm\{N(SiMe_3)\}_2$•$(THF)_2$ with an equimolar amount of $\{LO^{NO2}\}H$ only returned crystals of the dark green, homoleptic $\{LO^{NO2}\}_2Sm$ and of the colorless, trivalent $\{LO^{NO2}\}Sm\{N(SiMe_3)_2\}_2$ complexes which were characterized by XRD crystallography; it eventually proved impossible to obtain the desired $\{LO^{NO2}\}Sm\{N(SiMe_3)_2\}$ complex. Multiple attempts to obtain complexes akin to **3**-**4** by using protio-ligands having macrocyclic side-arms derived from 1-aza-12-c-4 or 1-aza-18-c-6 crown-ethers also failed; the protio-ligands could be made readily on multi-gram scales, but the macrocycles decomposed with detectable release of ethylene upon exposure to the very basic Ln(II) or Ae amido precursors. Note also that the clean synthesis of $\{LO^{NO4}\}Ca\{N(SiMe_3)_2\}$, *i.e.* the calcium derivative of **3**, could not be achieved due to systematic ligand redistribution in solution, giving mixtures of the target compound together with $[Ca\{N(SiMe_3)_2\}_2]_2$ and $\{LO^{NO4}\}_2Ca$.

The molecular solid-state structure of **7** depicted in Figure 1 features one of the four equivalent molecules found in the asymmetric unit. It shows a monometallic complex with a 6-coordinate calcium atom sitting in a much distorted octahedral geometry and κ^4-coordination of the aminoether-phenolate. All Ca–O and Ca–N bond distances in **7** are regular, and are for instance comparable to those in the related amido complex $\{LO^{NO2}\}Ca\{N(SiMe_2H)_2\}$•THF.[27] The Ca–C(41) bond length is substantially longer in **7** (2.570(4) Å) than in its precursor $Ca\{CH(SiMe_3)_2\}_2$•$(THF)_2$ (2.493(2) Å)[28] or in $Ca\{CH(SiMe_3)_2\}_2$•$(dioxane)_2$ (2.483(5) Å),[29] and compares better with that measured in the β-diketiminato complex $\{BDI^{iPr}\}Ca\{\eta^2\text{-}CH_2\text{-}2\text{-}(Me_2N)C_6H_4\}$ (2.535(4) Å; BDI^{iPr} = $CH[CMeN(2,6\text{-}^iPr_2\text{-}C_6H_3)]_2$).[25b]

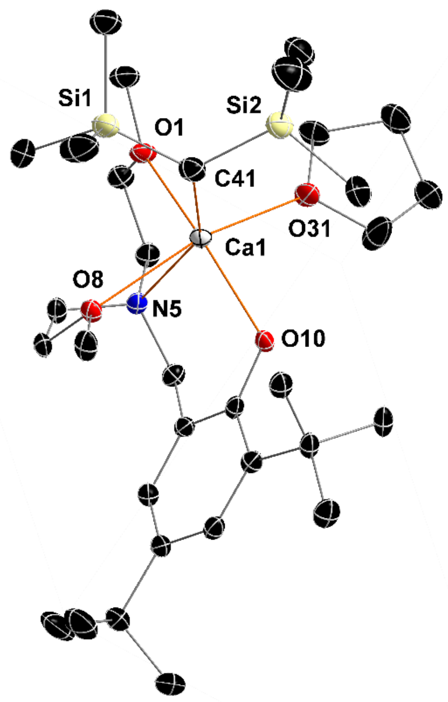

Figure 1. ORTEP representation of the molecular solid-state structure of $\{LO^{NO2}\}Ca\{CH(SiMe_3)_2\}$•THF (**7**). Ellipsoids drawn at the 30% probability level. H atoms are omitted for clarity. Selected bond lengths (Å): Ca1–O10 = 2.221(2), Ca1–O1 = 2.438(3), Ca1–O31 = 2.470(3), Ca1–O8 = 2.486(3), Ca1–N5 = 2.543(3), Ca1–C41 = 2.570(4).

The structure of **3** is displayed in Figure 2. It depicts a THF-free, monometallic complex with the ytterbium lying in a 7-coordinate environment. Amongst the main structural features, the Yb1–O1 distance of 2.277(2) Å to the $O_{phenolate}$ atom matches that in **2** (2.245(12 Å)), and it is a little longer than in the calcium congener $\{LO^{NO4}\}Ca\{N(SiMe_3)_2\}$, 2.211(2) Å.[27] However, the Yb1–N2 amido bond length in **3** (2.466(2) Å) is greater than in **2** (2.326(16) Å), the only other pertaining Yb(II)-phenolate complex reported to date.[11b] The elongated Yb–N_{amide} in **3** certainly reflects the greater coordination number of this complex, with a more electron-rich Yb(II) center resulting in a looser bond to the reactive amido group. The distances to the other nitrogen and oxygen atoms in **3** are unexceptional. The Yb^{2+} ion is too big to fit inside the crown-ether; instead, it rests 1.33 Å above the mean plane defined by the five heteroatoms in the side-arm macrocycle.

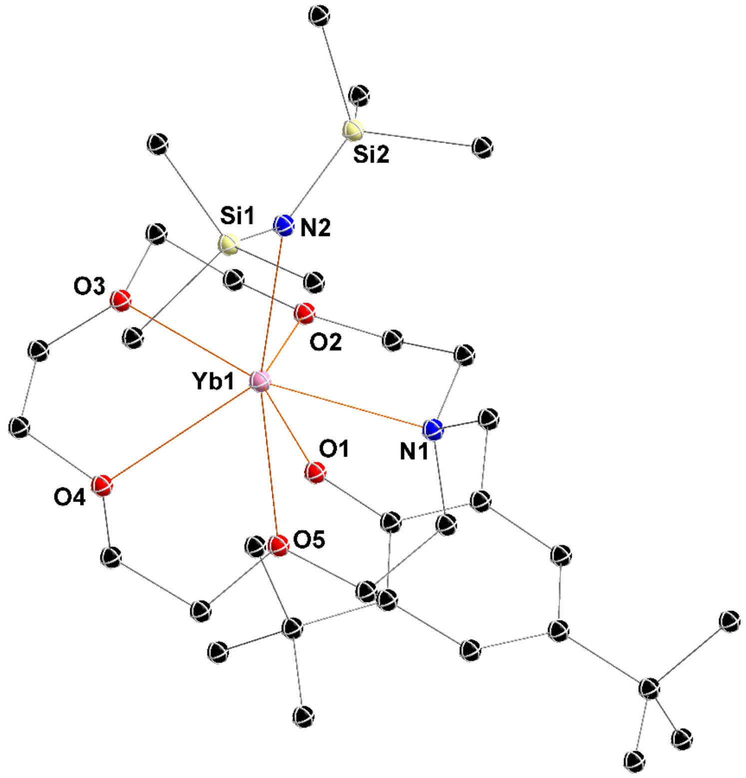

Figure 2. ORTEP representation of the molecular solid-state structure of $\{LO^{NO4}\}Yb\{N(SiMe_3)_2\}$ (**3**). Ellipsoids drawn at the 50% probability level. H atoms are omitted for clarity. Selected bond lengths (Å) and angles (°): Yb1–O1 = 2.277(2), Yb1–N2 = 2.466(2), Yb1–O2 = 2.481(2), Yb1–O3 = 2.615(2), Yb1–N1 = 2.633(3), Yb1–O5 = 2.705(2), Yb1–O4 = 2.712(2); Si2–N2–Yb1 = 134.18(14), Si1–N2–Yb1 = 100.98(11).

Hydrophosphination catalysis

The performances of the precatalysts **1-8** in the hydrophosphination of styrene with $PhPH_2$ ($[St]_0/[PhPH_2]_0/[Precat]_0$ = 50:50:1) were assessed in a preliminary screening. The data for $Yb\{N(SiMe_3)_2\}_2$•THF and $Sm\{N(SiMe_3)_2\}_2$•$(THF)_2$ were added to evaluate the importance of the aminoether-phenolates (Table 1, entries 1-2; no conversion was observed in either case after 1 h at 25 °C).[30] Representative data for experiments carried out at 25–60 °C in benzene-d_6 are collated in Table 1. Under the chosen experimental conditions, the reactions were very chemoselective, affording the secondary phosphine (*sec*-P) in >95% selectivity, that is, less than 5% of tertiary phosphine formed upon double (stepwise) hydrophosphination. The monohydrophosphination was regiospecific, generating exclusively the anti-Markovnikov product *sec*-P, with no indication for the formation of its regioisomer.

Table 1. Hydrophosphination of styrene with $PhPH_2$ catalyzed by **1**–**8**.[a]

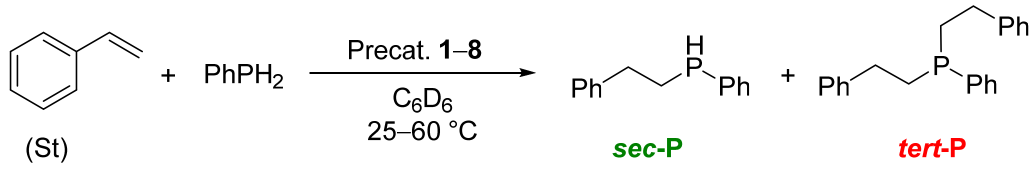

Run	Precatalyst	$[St]_0/[PhPH_2]_0/[Precat]_0$	T (°C)	t (h)	Conv. [b] (%)	*sec*-P/*tert*-P [c] (%)
1	$Yb\{N(SiMe_3)_2\}_2$•THF	50:50:1	60	24	8	99:1
2	$Sm\{(N(SiMe_3)_2\}_2$•$(THF)_2$	50:50:1	60	24	18	99:1
3	**1**	50:50:1	60	24	1	n.d.
4	**2**	50:50:1	60	24	52	99:1
5	**3**	50:50:1	60	0.5	100	94:6
6	**3**	50:50:1	25	1	74	97:3
7	**4**	50:50:1	60	0.5	80	97:3
8	**4**	50:50:1	25	1	63	97:3
9	**5**	50:50:1	60	24	24	97:3
10	**6**	50:50:1	60	24	40	99:1
11	**7**	50:50:1	60	24	34	99:1
12	**8**	50:50:1	60	24	15	100:0
13	**3**	100:100:1	25	3	72	99:1
14[d]	**3**	100:100:1	60	3	91	95:5
15[e]	**3**	200:200:1	60	3	82	96:4
16[f]	**3**	500:500:1	60	0.5	66	93:7
17[f]	**3**	500:500:1	60	15	100	93:7
18[g]	**3**	2,500:2,500:1	60	72	86	80:20
19	**3**	100:50:1	60	24	100	0:100
20[h]	**3**	100:100:1	25	3	100	99:1

[a] Reaction in benzene-d_6 (0.4-0.5 mL) with $[precat]_0$ = 11.5 mM unless otherwise specified. The formation of *sec*-P was 100% anti-Markovnikov regiospecific, as established by NMR spectroscopy. [b] Conversion of styrene, determined by NMR spectroscopy. [c] Product chemoselectivity determined by ^{31}P NMR spectroscopy. [d] $[precat]_0$ = 9.35 mM. [e] $[precat]_0$ = 7.95 mM. [f] $[precat]_0$ = 6.99 mM. [g] $[precat]_0$ = 1.62 mM. [h] Reaction performed in a Schlenk flask with permanent stirring.

Several trends emerge from entries 1−12 in Table 1: (*i*) the best two precatalysts are by a long margin the Ln(II) complexes **3** (Yb) and **4** (Sm) supported by the ligand $\{LO^{NO4}\}^{-}$ of highest denticity, the ytterbium one actually faring better (entries 5−8); (*ii*) for a given metal, the activity increases with the denticity of the ligand, compare entries 3, 4 and 5 for ytterbium, or entries 9 and 10 for calcium; (*iii*) with the tetradentate $\{LO^{ON2}\}^{-}$ ligand, the ytterbium(II) complexes are more efficient than their calcium analogues, compare entries 4 and 10−12. Note that **8** is not particularly efficient at 60 °C, presumably owing to its propensity for kinetic lability. The poor efficiency of the ytterbium(II) complex **1** (entry 3) in comparison with that of its calcium derivative **5** (entry 9) can be attributed to its limited solubility; (*iv*) the calcium alkyl and amido precatalysts **6** and **7** are equally competent; (*v*) the presence of the ancillary aminoether-phenolato ligand is required, as the bis(amido) compounds showed no catalytic activity under the chosen experimental conditions (entries 1−2). Note that issues linked to substrate diffusion might in some cases, *e.g.* entries 6 and 13, have limited the final conversion to ca. 70-75%; when performed in a Schlenk flask, complete conversion was observed (entry 20) where only 72% of 100 equivalents of each substrate had been converted in an NMR-scale reaction (entry 13).

Further reactions were carried out with the best precatalyst, **3** (entries 13−19). It proved robust enough to withstand as much as 2,500 equiv of each substrate (entry 18), achieving 86% conversion (overall turnover TON = 2,150; apparent turnover frequency TOF = 30 h^{-1}) after 72 h, although the final chemoselectivity was lower under such demanding conditions requiring longer reaction times. With up to 500 equiv of substrates, excellent conversions and chemoselectivity were observed, and the reaction times remained reasonably short (entries 13−17). Interestingly, with a $[\text{styrene}]_0/[PhPH_2]_0/[\mathbf{3}]_0$ = 100:50:1 initial ratio, the formation of the tertiary phosphine *tert*-P was quantitative and selective after 24 h (entry 19).

To take advantage this last feature, **3** was employed for the one-pot, two-step synthesis of unsymmetrical tertiary phosphines having three different substituents on the phosphorus atom (Scheme 2). The set of experiments was performed in benzene-d_6 at 25 °C. A reaction time of 2 h for the equimolar hydrophosphination of $PhPH_2$ with styrene ($[styrene]_0/[PhPH_2]_0/[\mathbf{3}]_0$ = 50:50:1) enabled quantitative conversion of the first load of substrates. A second batch of styrene derivative was then added to this reaction mixture (50 equiv vs. **3**). A series of such experiments were conducted with different substituents in the *para* position (X = Cl, F, ^{t}Bu, OMe) of the styrenic substrate. As with styrene (X = H), for the *p*-Cl and *p*-F derivatives the second phase of the process was completed within 3 h, neatly affording original asymmetric phosphines in quantitative yields. The reaction was slower with the *p*-^{t}Bu substituent, the conversion reaching 56% in 20 h, whereas it did not proceed further with the very electron-donating *p*-OMe substituent. The reaction rate is hence sensitive to electronic effects in the styrenic substrate, and varied according to OMe < ^{t}Bu < H, F, Cl.

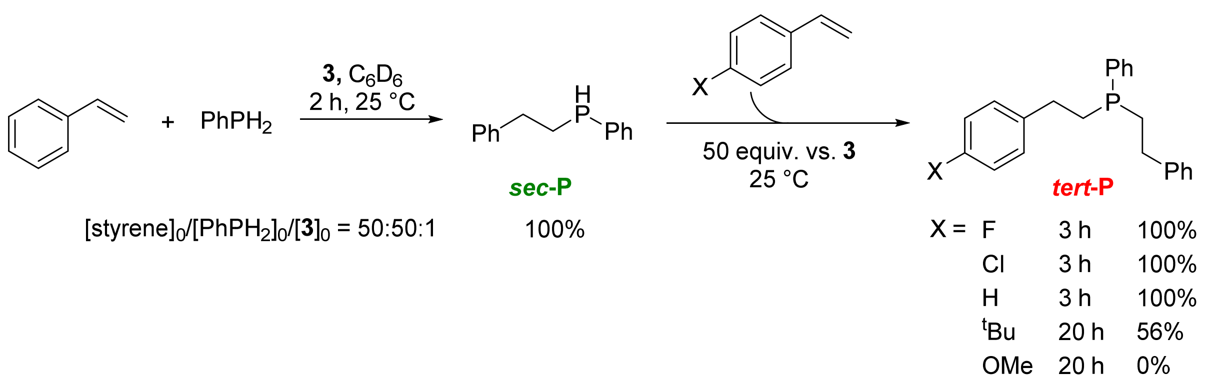

Scheme 2. Synthesis of tertiary phosphines by one-pot, two-step reaction catalyzed by **3**.

Kinetic analysis

Kinetic monitoring was performed by ^{1}H NMR spectroscopy. The reactions were carried out in benzene-d_6, using precatalyst **3**. The hydrophosphination between $PhPH_2$ and *p*-^{t}Bu-styrene, a substrate which lends itself well to the monitoring of substrate conversion, was first examined. At 25 °C, in the presence of a 3 to 5-fold excess of p-^{t}Bu-styrene vs. $PhPH_2$, the plot of the conversion of $PhPH_2$ vs. reaction time was linear (Figure 3), indicating a zeroth-order dependence in [$PhPH_2$]. Conversely, with a 3 to 10-fold excess of $PhPH_2$, the semi-logarithmic plots of the concentration in p-^{t}Bu-styrene vs. reaction time were linear (Figure 4), showing a first-order dependence in [p-^{t}Bu-styrene]. On the other hand, the corresponding observed rate constants k_{obs} decreased linearly from $4.3170(1)\cdot10^{-5}$ s^{-1} to $2.9830(1)\cdot10^{-5}$ s^{-1} with increasing p-^{t}Bu-styrene concentration (Figure 5). This is indicative of catalyst inhibition by this substrate probably by formation of an adduct as an off-cycle species; this suggests that the rate-limiting insertion of the C=C bond into the Yb–P bond (*vide infra*) first requires the dissociation of molecules of p-^{t}Bu-styrene from the Lewis acidic ytterbium(II) cation. Relevant occurrences of catalyst inhibition by the substrate have been reported for the cyclohydroamination of aminoalkenes[31] and for the hydroalkoxylation/cyclization of alkynyl alcohol[32] catalyzed by alkaline-earth complexes.

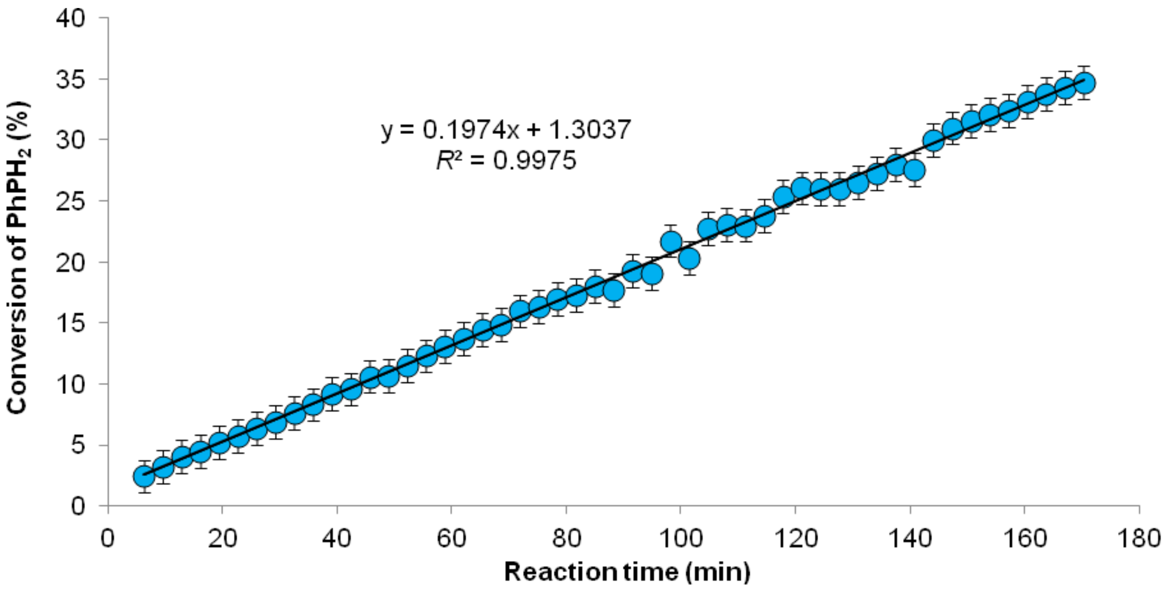

Figure 3. Conversion of $PhPH_2$ vs. reaction time for the hydrophosphination of p-^{t}Bu-styrene catalyzed by $\{LO^{NO4}\}Yb\{N(SiMe_3)_2\}$ (**3**) in benzene-d_6. Reaction conditions: $[PhPH_2]_0$/[p-^{t}Bu-styrene]$_0$/[**3**]$_0$ = 30:100:1, with [**3**]$_0$ = 18.0 mM; T = 25 °C; total volume = 0.6 mL.

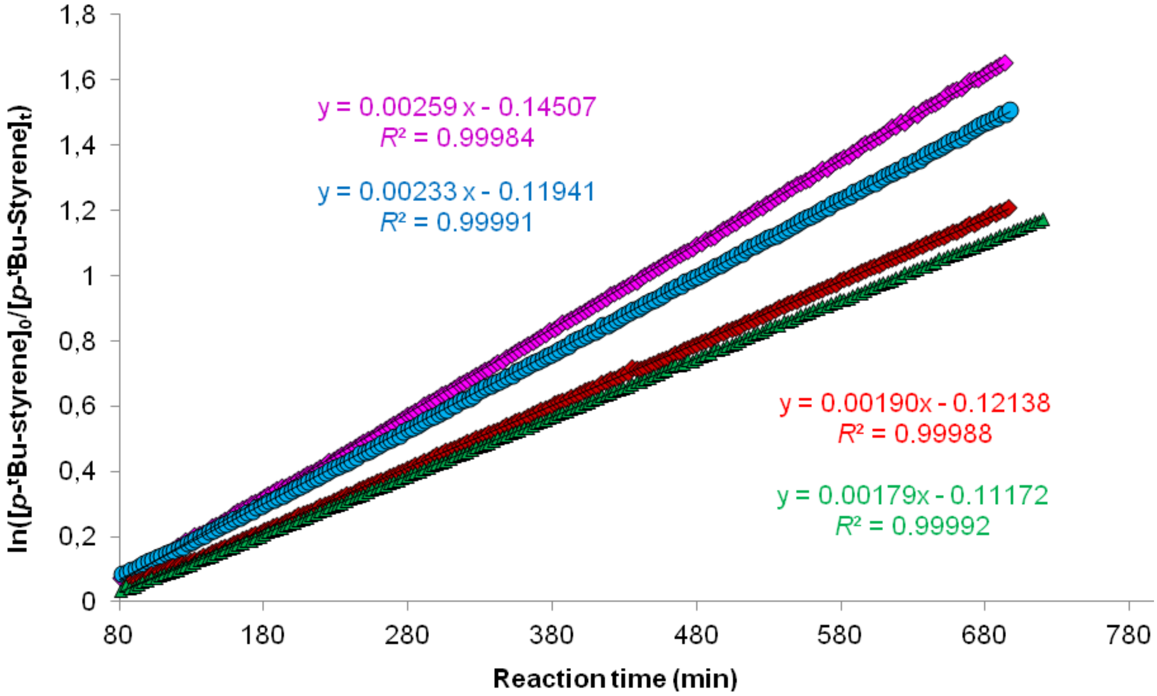

Figure 4. Semi-logarithmic plot of ln([*p*-^{t}Bu-Styrene]$_0$/[*p*-^{t}Bu-Styrene]$_t$) vs. reaction time for the hydrophosphination of *p*-^{t}Bu-Styrene with $PhPH_2$ catalyzed by {LO^{NO4}}Yb{N(SiMe$_3$)$_2$} (**3**) in benzene-d_6. Reaction conditions: [$PhPH_2$]$_0$/[*p*-^{t}Bu-styrene]$_0$/[**3**]$_0$ = 100:X:2.5, with [**3**]$_0$ = 45.0 mM; T = 25 °C; total volume = 0.6 mL. X = 10 (◆), 15 (●), 25 (◆), 30 (▲) equiv.

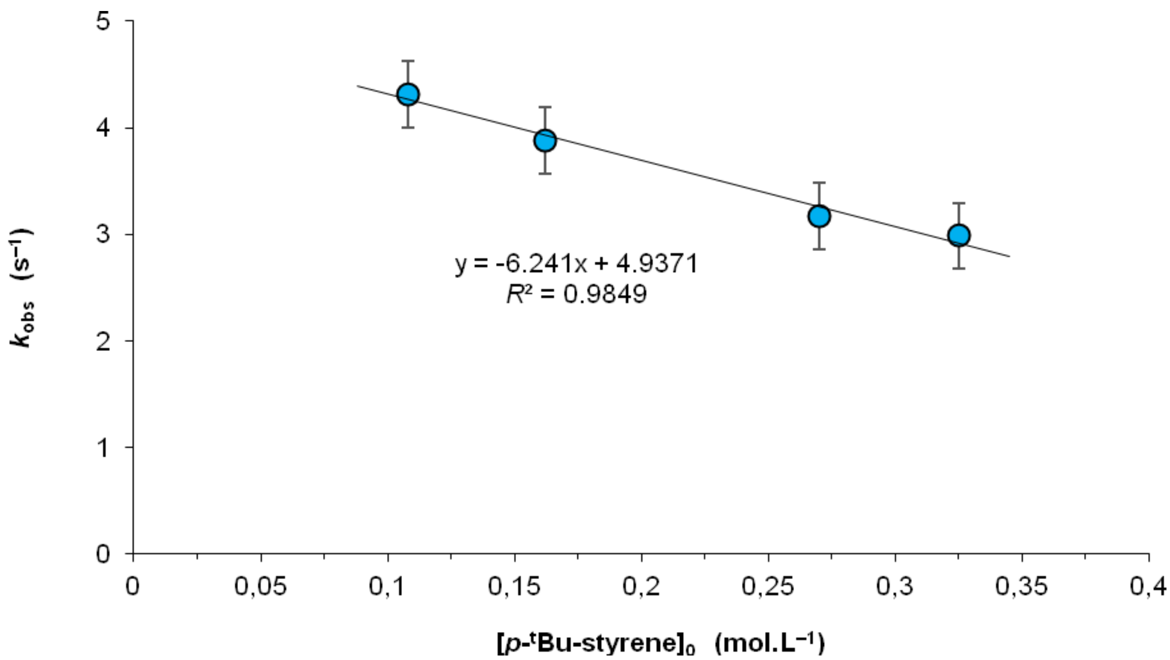

Figure 5. Plot of the observed rate constant vs. concentration in *p*-^{t}Bu-styrene for the hydrophosphination of *p*-^{t}Bu-Styrene with $PhPH_2$ catalyzed by {LO^{NO4}}Yb{N(SiMe$_3$)$_2$} (**3**) in benzene-d_6. Reaction conditions: [$PhPH_2$]$_0$/[*p*-^{t}Bu-styrene]$_0$/[**3**]$_0$ = 100:X:2.5, with [**3**]$_0$ = 45.0 mM; T = 25 °C; total volume = 0.6 mL, X = 10, 15, 25, 30 equiv.

A partial kinetic order of 1 in precatalyst concentration [**3**] was determined from the plot of ln(k_{obs}) vs. ln([**3**]), when the concentration in **3** was increased from 10.8 to 43.3 mM while keeping the concentrations in the substrates constant (Figure 6); this was confirmed by plotting the variation of the observed first-order rate constant k_{obs} vs. $[\mathbf{3}]_0$, which was also a straight line (Figure 7). The rate law for the hydrophosphination of *p*-^{t}Bu-styrene with $PhPH_2$ catalyzed by **3** therefore agrees to the idealized equation (1):

$$Rate = k.[p\text{-}^t\text{Bu-styrene}]^1.[\mathbf{3}]^1 \qquad (1)$$

The activation parameters $\Delta H^‡ = 7.2$ kcal·mol^{-1} and $\Delta S^‡ = -46.4$ cal·mol^{-1}·K^{-1} were determined for the reaction by Eyring analysis performed in the temperature range 25 to 75 °C (Figure 8). This corresponds to a $\Delta G^‡$ value of 21.0 kcal·mol^{-1} at 25 °C. These values indicate that the reaction is essentially controlled by a high entropic barrier, with an associative mechanism involving a very ordered transition state. Occurrences of large activation entropy such as that observed here have been mentioned before. It has been reported in other pioneering computational and kinetic works in thiourea catalysis,[33] or in the metal-templated synthesis of [3]-rotaxanes.[34] In our case, it may perhaps be linked to substantial stiffening of the otherwise very flexible ligand aza-crown-ether side-arm in the transition state, although we cannot provide evidence to support this claim.

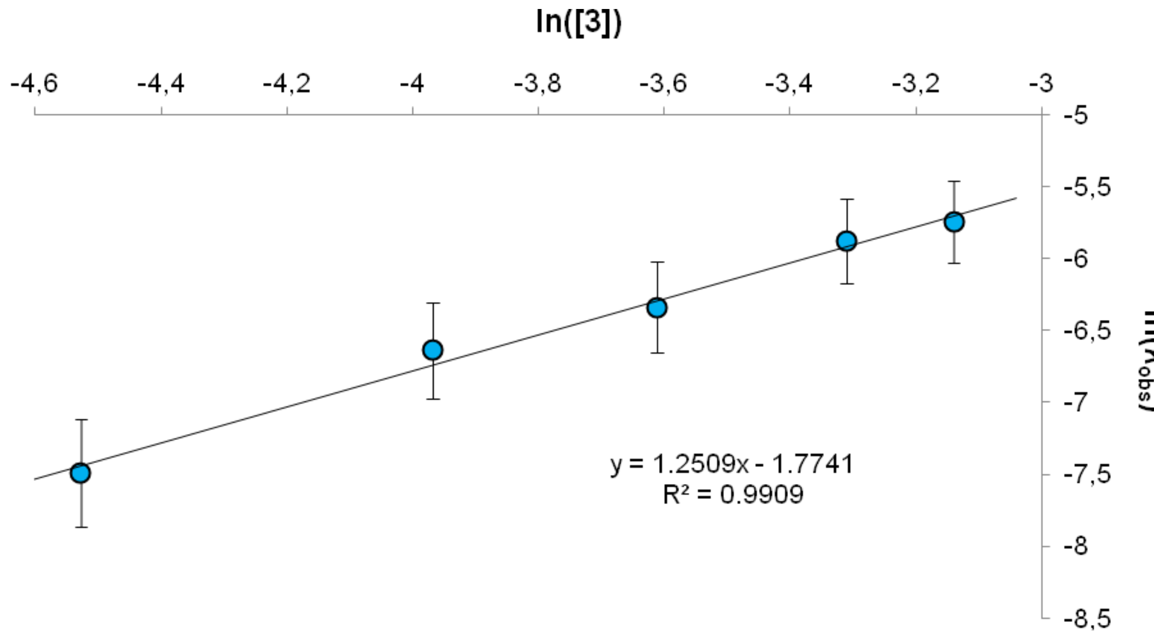

Figure 6. Plot of ln(k_{obs}) vs. ln([**3**]) for the hydrophosphination of *p*-^{t}Bu-Styrene with $PhPH_2$ catalyzed by {LO^{NO4}}Yb{N($SiMe_3$)$_2$} (**3**) in benzene-d_6. Reaction conditions: [$PhPH_2$]$_0$/[*p*-^{t}Bu-styrene]$_0$/[**3**]$_0$ = 100:25:X; T = 25 °C; [$PhPH_2$]$_0$ = 1.08 mM, /[*p*-^{t}Bu-styrene]$_0$ = 0.27 mM; total volume = 0.6 mL; [**3**]$_0$ = 10.8, 18.9, 27.0, 35.5 and 43.3 mM.

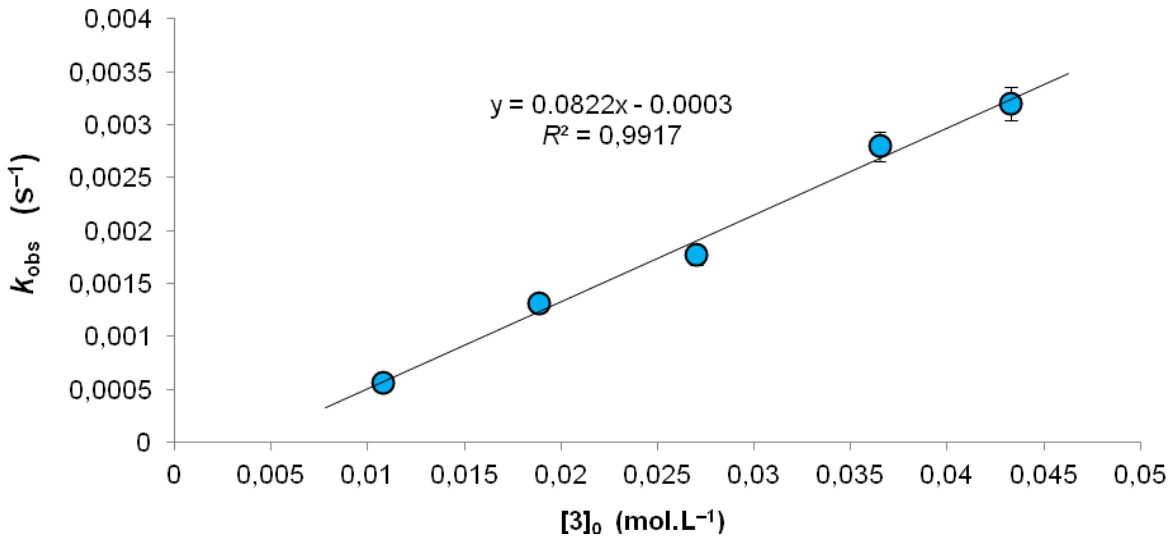

Figure 7. Plot of k_{obs} vs. [**3**]$_0$ for the hydrophosphination of *p*-^{t}Bu-Styrene with $PhPH_2$ catalyzed by {LO^{NO4}}Yb{N($SiMe_3$)$_2$} (**3**) in benzene-d_6. Reaction conditions: [$PhPH_2$]$_0$/[*p*-^{t}Bu-styrene]$_0$/[**3**]$_0$ = 100:25:X; T = 25 °C; [$PhPH_2$]$_0$ = 1.08 mM, [*p*-^{t}Bu-styrene]$_0$ = 0.27 mM; total volume = 0.6 mL; [**3**]$_0$ = 10.8, 18.9, 27.0, 35.5 and 43.3 3 mM.

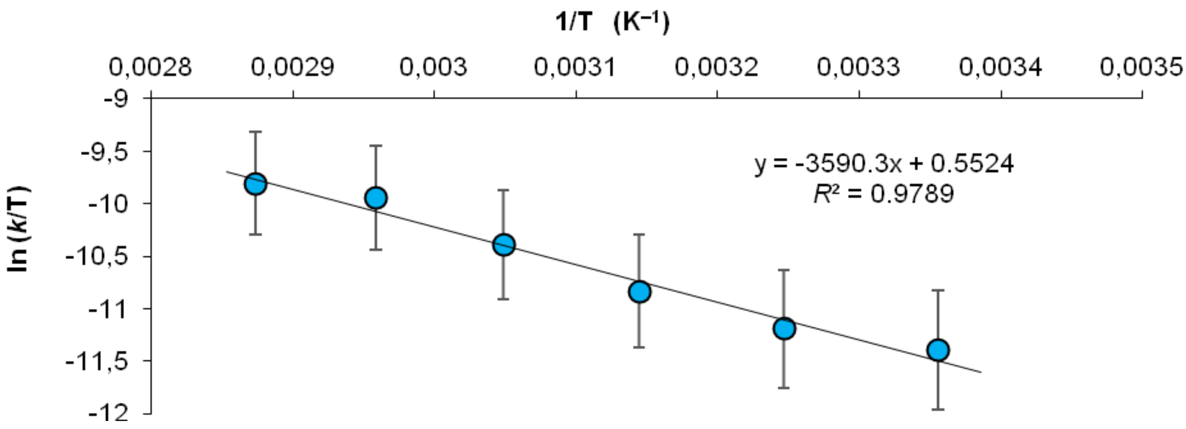

Figure 8. Eyring plot for the hydrophosphination of *p*-^{t}Bu-Styrene with $PhPH_2$ catalyzed by $\{LO^{NO4}\}Yb\{N(SiMe_3)_2\}$ (**3**) in benzene-d_6, in temperature range 25–75 °C. $[PhPH_2]_0/[p\text{-}^t\text{Bu-styrene}]_0/[\mathbf{3}]_0$ = 25:25:1; total volume = 0.6 mL; $[\mathbf{3}]_0$ = 36.0 mM.

The influence of the substituent in styrene derivatives mentioned above was probed in more detail by monitoring the kinetics for the hydrophosphination between $PhPH_2$ and substituted *para*-X-styrene derivatives (*p*-X-styrene, with X chosen amongst CF_3, F, Cl, Br, H, ^{t}Bu, Me, OMe) or *meta*-OMe-styrene. With *p*-CF_3-styrene, the immediate formation of a black precipitate indicative of catalyst decomposition was seen, presumably by reaction between the complex and the fluorinated group. From the plots given in Figure 9, the observed zero-order rate constants k_{obs} can be deduced immediately. The reactions with *p*-Cl-styrene and *p*-Br-styrene were very fast and only a few data points could be recorded before full conversion. Figure 9 confirms that reaction rates globally increase with the Hammett σ constant of the substituents (except for the peculiarly low rate observed for *p*-F) with the sequence *p*-OMe (σ_p = –0.27) < *p*-^{t}Bu (σ_p = –0.20) < *p*-Me (σ_p = –0.17) < *p*-F (σ_p = 0.06) < *p*-H (σ_p = 0) < *m*-OMe (σ_m = 0.12) < *p*-Br (σ_p = 0.23) ≈ *p*-Cl (σ_p = 0.23).[35] The lower reaction rates observed for *p*-F-styrene as compared with styrene are surprising, but the reproducibility between independent tests was excellent; it must reflect a concrete experimental fact or mechanistic feature which we cannot rationalize at this time.[36] That the reaction rates overall increase with the Hammett σ constants of the substituents on the aromatic ring in the styrene derivatives suggests that bond polarization occurs, with a transition state having a negative charge developing on the carbon atom in α position to the aromatic ring. This replicates the scenario known for alkalino-earth catalysts.[10] Based on this analogy with Ae-catalysis and the rate law in equation (1), we propose that these hydrophosphination reactions proceed by turnover-limiting olefin insertion into the [Yb]–phosphide bond (Scheme 3). The tailing off observed in the reactions with styrene (X = H) may be due to a concentration gradient which slows reactivity in the J-Young NMR tube, as mentioned previously (Table 1, entries 6, 13 and 20).

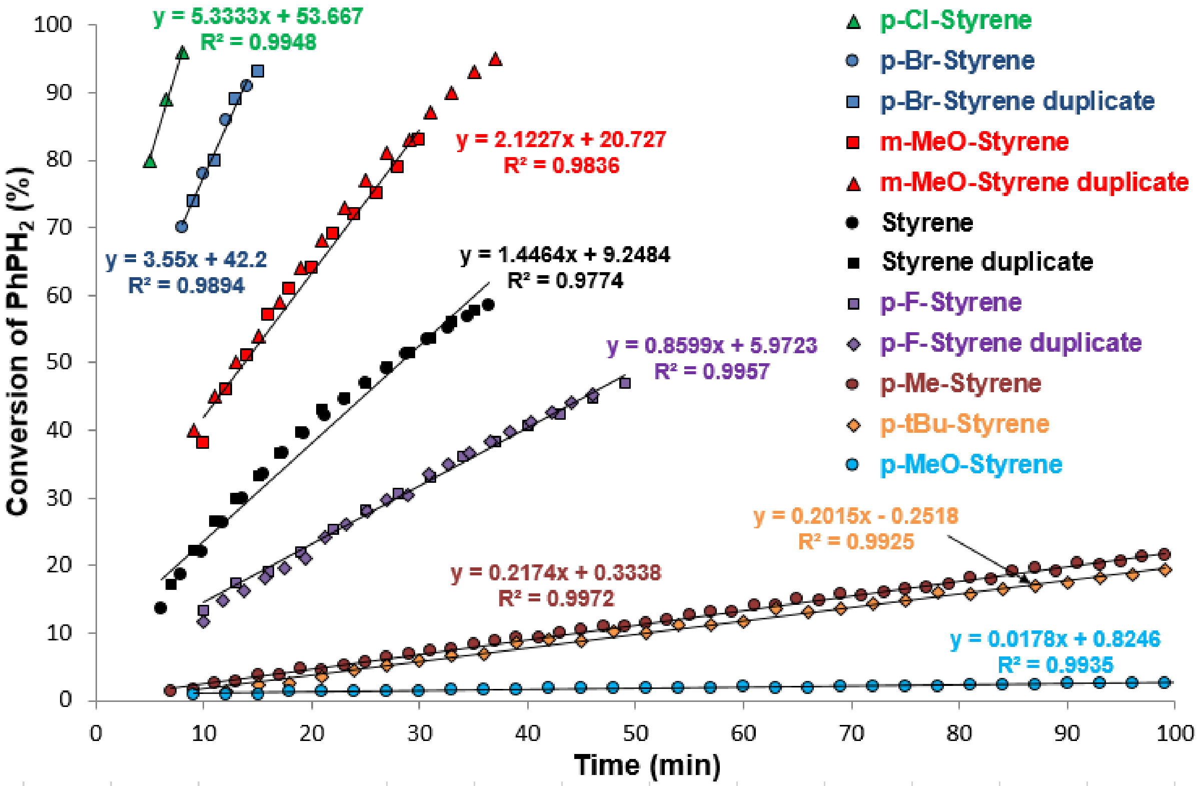

Figure 9. Plot of $PhPH_2$ conversion vs. reaction time for the hydrophosphination of *p*-X-styrene catalyzed by $\{LO^{NO4}\}Yb\{N(SiMe_3)_2\}$ (**3**) in benzene-d_6. $[PhPH_2]_0/[p\text{-X-styrene}]_0/[\mathbf{3}]_0$ = 25:25:1; T = 25 °C; total volume = 0.6 mL; $[\mathbf{3}]_0$ = 36.0 mM. X = Cl, H, F, Me, ^{t}Bu or OMe.

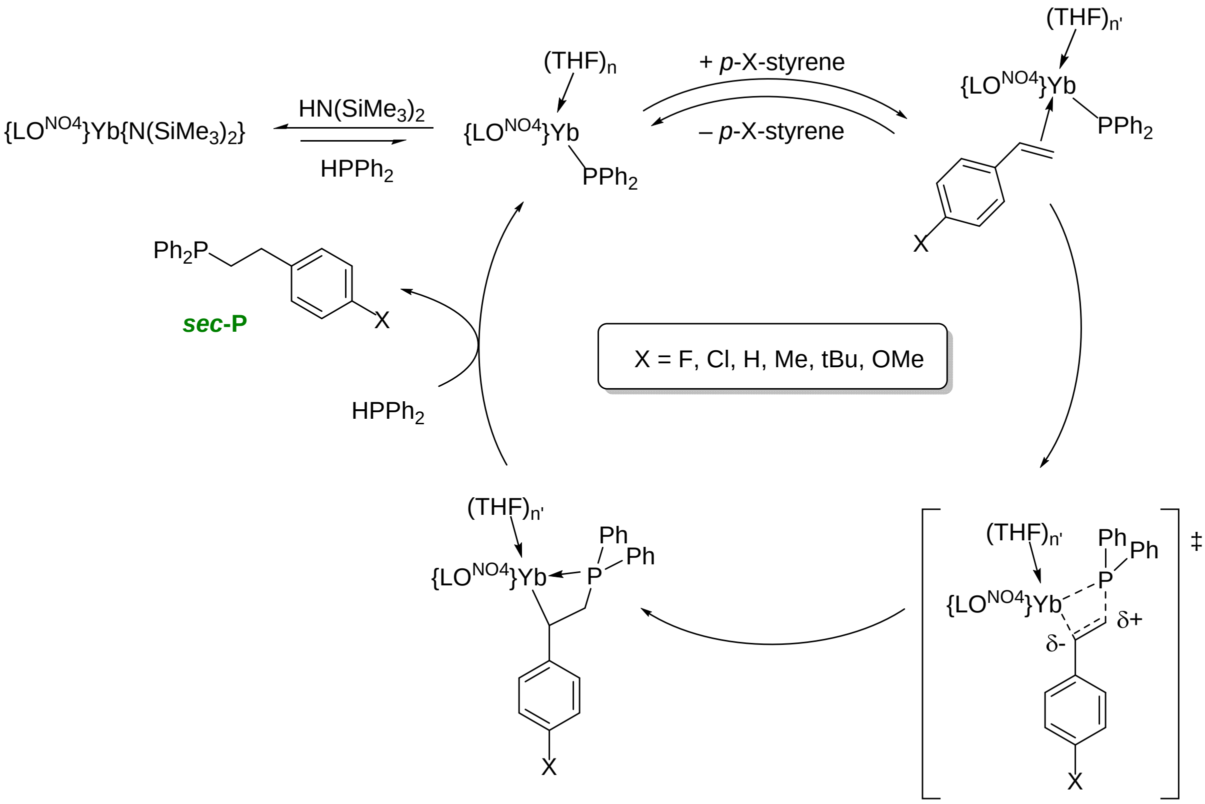

Scheme 3. Proposed mechanism for the hydrophosphination of styrene derivatives with $PhPH_2$ catalyzed by Ln(II) precatalysts, illustrated here with **3**.

Consecutive hydrophosphinations

The kinetics of the catalyzed reaction between *p*-^{t}Bu-styrene and *two* equiv of $PhPH_2$ leading to the formation of the secondary (*sec*-P) and tertiary (*tert*-P) phosphines by mono- and dihydrophosphination, respectively, were monitored to inform ourselves about the chemoselectivity of this process. The reaction was carried out in benzene-d_6 at 25 °C, with $[PhPH_2]_0/[p\text{-X-styrene}]_0/[\mathbf{3}]_0$ = 25:50:1, with $[\mathbf{3}]_0$ = 72.2 mM. The plot displayed in Figure 10 is rich of information. The kinetic profile for the concentrations in the various phosphines is not typical of consecutive reactions.[37]

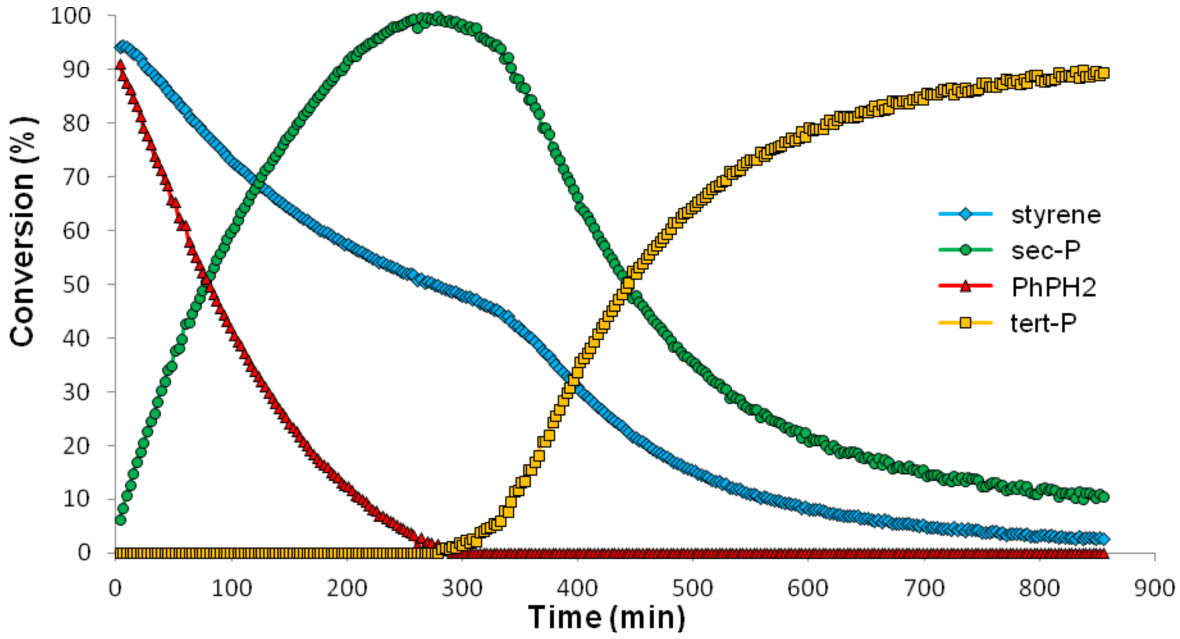

Figure 10. Plot of reagent conversion vs. reaction time for the hydrophosphination of *p*-^{t}Bu-Styrene with $PhPH_2$ catalyzed by $\{LO^{NO4}\}Yb\{N(SiMe_3)_2\}$ (**3**) in benzene-d_6 at 25 °C. $[PhPH_2]_0/[p\text{-}^{t}Bu\text{-styrene}]_0/[\mathbf{3}]_0$ = 25:50:1; total volume = 0.6 mL; $[\mathbf{3}]_0$ = 72.2 mM.

The formation of *sec*-P is fully chemospecific, and it is *only* when the whole of $PhPH_2$ has been converted into *sec*-P that the formation of *tert*-P begins, after nearly 5 h. As expected owing to the zeroth-order dependence in $[PhPH_2]$, the rate of consumption of $PhPH_2$ is linear for at least 120 min, at which point a regime of substrate depletion is reached. The rate of consumption of styrene in the first phase (corresponding to the formation of *sec*-P, t < 300 min) *and* in its second phase (formation of *tert*-P, t > 300 min) shows the expected first-order dependence in [*p*-^{t}Bu-styrene]. Remarkably, they exhibit observed rate constants that are commensurate, $k_{obs,1}$ = $4.667(1)\cdot10^{-5}$ s^{-1} and $k_{obs,2}$ = $11.500(1)\cdot10^{-5}$ s^{-1}, respectively. Similarly, the rate of consumption of *sec*-P in the second phase (k_2 = $6.815(1)\cdot10^{-3}$ $mol.L^{-1}.s^{-1}$) is comparable to that measured during the first phase for the conversion of $PhPH_2$ (k_1 = $8.275(1)\cdot10^{-3}$ $mol.L^{-1}.s^{-1}$). In other words, the rates of the reaction of a primary ($PhPH_2$) and a secondary (*sec*-P) phosphine with *p*-^{t}Bu-styrene are very similar. On this basis, it is remarkable that the formation of *tert*-P only starts occurring when complete consumption of $PhPH_2$ and quantitative formation of *sec*-P are ensured, after ca. 300 min. These events are also concomitant with a reacceleration of the rate of consumption of *p*-^{t}Bu-styrene (blue trace in Figure 10). These observations strongly suggest that, although the secondary phosphine is competitive in terms of kinetics, the σ-bond metathesis of the reaction intermediate with the secondary phosphine is much slower than that with the primary phosphine.

■ CONCLUSION

Ytterbium(II) aminoether-phenolato complexes constitute very competent precatalysts for the intermolecular hydrophosphination of activated alkenes, illustrated here in the case of styrenic substrates. The catalyzed reactions also work for conjugated dienes, *e.g.* isoprene, but the reactivity of the catalyst is not sufficient to warrant the hydrophosphination of *unactivated* alkenes. For instance, the hydrophosphination of 1-nonene with $PhPH_2$ catalyzed by **3** only reaches 3% conversion after 70 h at 60 °C. Perhaps this situation could be improved by preparing alkyl derivatives of **3**, and we are working in this aim. In the meantime, Waterman's zirconium alkyl-amido complex remains unique with this respect.[9b]

The differences between alkalino-earth metals and divalent lanthanides in this very catalysis are plain, with in particular ytterbium(II) clearly surpassing the more common Ae, and especially calcium, precatalysts. With these ytterbium(II) aminoether-phenolato species, the catalytic activity increases substantially with the denticity of the ligand. The opposite was found in the Ae-mediated hydroamination of aminoalkenes,[38] whereas there was no clear trend in Ae-promoted intermolecular alkene hydrophosphination.[10b-c]

One of the most salient properties of these ytterbium(II) hydrophosphination precatalysts, and amongst these most prominently the kinetically stabilized $\{LO^{NO4}\}Yb\{N(SiMe_3)_2\}$ (**3**), is their chemoselectivity towards the production of secondary or tertiary phosphines. The unusual reactivity and kinetic profile which characterize the double hydrophosphination are remarkable features that enable the preparation of a virtually boundless range of valuable asymmetric tertiary phosphines starting from primary phosphines such as the archetypal $PhPH_2$. Future efforts should focus on rendering this process enantioselective.

■ EXPERIMENTAL SECTION

General procedures. NMR spectra were recorded on Bruker AC-400 and AM-500 spectrometers. All chemicals ^1H and ^{13}C shifts were determined using residual signals of the deuterated solvents and were calibrated *vs*. $SiMe_4$. Assignment of the signals was carried out using 1D (^1H, $^{13}C\{^1H\}$) and 2D (COSY, HMBC, HMQC) NMR experiments. ^{31}P NMR spectra were calibrated *vs*. phosphoric acid. All coupling constants are given in Hertz. Elemental analyses were performed on a Carlo Erba 1108 Elemental Analyser instrument at the London Metropolitan University by Stephen Boyer and were the average of a minimum of two independent measurements. $HN(SiMe_3)_2$ (Acros) was dried over activated 3 Å molecular sieves and distilled under reduced pressure prior to use. Solvents (THF, Et_2O, CH_2Cl_2, pentane and toluene) were purified and dried (water contents all below 6 ppm) over alumina columns (MBraun SPS). THF was further distilled under argon from sodium mirror/benzophenone ketyl prior to use. All deuterated solvents (Eurisotop, Saclay, France) were stored in sealed ampoules over activated 3 Å molecular sieves and were thoroughly degassed by several freeze-thaw cycles. The precursors $Ln\{N(SiMe_3)_2\}_2(THF)_x$ (Ln = Yb, x = 1; Sm, x = 2),[39] $Ca\{CH(SiMe_3)_2\}_2•(THF)_2$[28] and the aminoether-phenol protio-ligands[24] were prepared as described elsewhere. The syntheses of the divalent lanthanide **1-4**[11b] and alkalino-earth **5-6**[24] were reported previously, and the readers are referred to the relevant articles for all synthetic and characterization details. Despite repeated attempts performed on crystalline samples from different batches, satisfactory elemental analysis could not be obtained for compounds **7** and **8**, most probably because of their extreme and moisture sensitivity. Styrenic substrates (Acros / Aldrich) were vacuum-distilled over CaH_2 and then degassed by freeze-pump-thaw methods. Phenylphosphine was purchased from Aldrich and used as received.

X-ray diffraction crystallography. Diffraction data for complex **7** (CCDC 1468793) were collected at 150(2) K using a Bruker APEX CCD diffractometer with graphite-monochromated MoKα radiation (λ = 0.71073 Å). A combination of ω and Φ scans was carried out to obtain at least a unique data set. The crystal structures were solved by direct methods, remaining atoms were located from difference Fourier synthesis followed by full-matrix least-squares refinement based on F2 (programs SIR97 and SHELXL-97).[40] Many hydrogen atoms could be found from the Fourier difference analysis. Carbon-bound hydrogen atoms were placed at calculated positions and forced to ride on the attached atom. The hydrogen atom contributions were calculated but not refined. All non-hydrogen atoms were refined with anisotropic displacement parameters. The locations of the largest peaks in the final difference Fourier map calculation as well as the magnitude of the residual electron densities were of no chemical significance. The crystallographic data for **3** (CCDC 1045763) were collected on a Xcalibur Eos diffractometer (graphite monochromated, MoKα radiation, ω-scan technique, λ = 0.71073 Å, T = 100(2) K). Its structure was solved by direct methods and was refined on F^2 using the SHELXTL v. 6.12 package.[41] All non-hydrogen atoms were found from Fourier syntheses of electron density and were refined anisotropically. All hydrogen atoms were placed in calculated positions and were refined in the riding model. SCALE3 ABSPACK[42] was used to perform area detector scaling and absorption corrections. Relevant collection and refinement data for all compounds are given in the Supporting information. All data can be obtained from the Cambridge Structural Database via www.ccdc.cam.ac.uk/data_request/cif.

Hydrophosphination experiments. In a typical reaction with neat substrates, the precatalyst was loaded in an NMR tube in the glove-box. *p*-^{t}Bu-styrene and $PhPH_2$ were then added in and the reaction time started after quickly placing the NMR tube in an oil bath preheated at the desired temperature. After the desired reaction time, the NMR tube was open to air, non-dried benzene-d_6 was added to the reaction mixture, and the ^{1}H NMR spectrum was recorded. Conversion was determined by integrating the remaining *p*-^{t}Bu-styrene and the newly formed addition product. Reactions in dry benzene-d_6 were carried out in similar manner, but adding the solvent at the same time as the substrates to the NMR tube.

{LO^{NO2}}CaCH(SiMe$_3$)$_2$•THF (7). At room temperature, a solution of {LO^{NO2}}H (0.35 g, 1.00 mmol) in pentane (10 mL) was added slowly to a solution of Ca{CH(SiMe$_3$)$_2$}$_2$•(THF)$_2$ (0.52 g, 1.03 mmol) in pentane (10 mL). After 6 h, the reaction solution was concentrated to 5 mL, giving a white precipitate which was isolated by filtration. The resulting powder was dried in vacuo to constant weight to afford **7** as a colorless powder (0.40 g, 70%). Single-crystals suitable for X-ray diffraction crystallography were obtained by recrystallization from a concentrated pentane/benzene mixture. ^{1}H NMR (benzene-d_6, 298 K, 500.13 MHz): δ 7.58 (d, $^4J_{HH}$ = 2.4 Hz, 1H, *m*-H), 6.96 (d, $^4J_{HH}$ = 2.4 Hz, 1H, *m*-H), 3.60 (m, 4H, THF), 3.16 (br s, 2H, Ar-C*H*$_2$N), 2.97 (s, 6H, OC*H*$_3$), 2.73 (m, 2H, CH$_2$C(*H*)HO), 2.63 (m, 2H, CH$_2$C(*H*)HO), 2.02 (m, 2H, NC*H*$_2$CH$_2$), 1.83 (m, 2H, NC*H*$_2$CH$_2$, overlapping with s, 9H, *o*-C(C*H*$_3$)$_3$), 1.48 (s, 9H, *p*-C(C*H*$_3$)$_3$), 1.40 (m, 4H, THF), 0.47(s, 18H, Si(C*H*$_3$)$_3$), –1.87 (s, 1H, C*H*Si(CH$_3$)$_3$) ppm. ^{13}C{^{1}H} NMR (benzene-d_6, 298 K, 125.76 MHz): δ 164.8 (*i*-C), 137.6 (*o*-C), 126.2 (*p*-C), 124.9 (*m*-C), 70.4 (CH$_2$*C*H$_2$O), 68.7 (THF), 60.4 (O*C*H$_3$), 58.2 (Ar*C*H$_2$N), 54.3 (N*C*H$_2$CH$_2$), 36.3 (*o*-*C*(CH$_3$)$_3$), 34.9 (*p*-*C*(CH$_3$)$_3$), 32.9 (*p*-C(*C*H$_3$)$_3$), 31.0 (*o*-C(*C*H$_3$)$_3$), 26.1 (THF), 6.8 (Si(*C*H$_3$)$_3$), 1.9 (*C*HSi(CH$_3$)$_3$) ppm.

$\{LO^{NO2}\}Sr\{CH(SiMe_3)_2\}$ (8). Following the same procedure as that described for **7**, $\{LO^{NO2}\}H$ (0.40 g, 1.14 mmol) was reacted with $Sr\{CH(SiMe_3)_2\}_2$•$(THF)_3$ (0.73 g, 1.17 mmol) to give **8** as a white powder (0.38 g, 55%). ^1H NMR (THF-d_8, 298 K, 500.13 MHz): δ 7.08 (s, 1H, *m*-H), 6.75 (s, 1H, *m*-H), 3.58 (overlapping br, 2H, ArCH_2N + s, 2H, CH_2O), 3.52 (br s, 2H, CH_2O), 3.47 (s, 6H, OCH_3), 2.70 (br s, 2H, NCH_2CH$_2$), 2.63 (br s, 2H, NCH_2CH$_2$), 1.43 (s, 9H, *o*-C(CH_3)$_3$), 1.22 (s, 9H, *p*-C(CH_3)$_3$), 0.03 (s, 18H, Si(CH_3)$_3$), –2.20 (s, 1H, C*H*Si(CH$_3$)$_3$) ppm. $^{13}C\{^1H\}$ NMR (THF-d_8, 298 K, 125.76 MHz): δ 166.5 (*i*-C), 136.4 (*o*-C), 131.9 (*p*-C), 126.8 (*o*-C), 124.0 (*m*-C), 123.6 (*m*-C), 71.7 (*C*H$_2$O), 69.9 (*C*H$_2$O), 60.3 (O*C*H$_3$), 60.1 (Ar*C*H$_2$N), 54.6 (N*C*H$_2$CH$_2$), 36.1 (*o*-*C*(CH$_3$)$_3$), 34.5 (*p*-*C*(CH$_3$)$_3$), 32.7 (*p*-C(*C*H$_3$)$_3$), 30.7 (*o*-C(*C*H$_3$)$_3$), 6.6 (Si(*C*H$_3$)$_3$), 1.7 (*C*HSi(CH$_3$)$_3$), ppm.

■ ASSOCIATED CONTENTS

XRD structures of **3** and **7** added as CIF files. ^1H NMR spectra for monitored catalyzed reactions.

■ AUTHOR INFORMATION

Corresponding Authors

*E-mail: jean-francois.carpentier@univ-rennes1.fr; yann.sarazin@univ-rennes1.fr; trif@iomc.ras.ru

Notes

The authors declare no competing financial interest.

■ ACKNOWLEDGMENTS

This work was sponsored by the Russian Foundation for Basic Research (Grant 15-33-20285), by a Grant of President of Russian Federation for young scientists (grant no. MK-5702.2015.3), by the GDRI CNRS-RAS "Homogeneous Catalysis for Sustainable Development", and by the European Union (grant FP7-People-2010-IIF *ChemCatSusDe* to B. L.)

■ NOTES AND REFERENCES

1 For reviews, see: (a) Wicht, D. K.; Glueck, D. S. in *Catalytic Heterofunctionalization* (Eds.: A. Togni, H. Grützmacher), Wiley-VCH: Weinheim, **2001**, pp. 143-170. (b) Tanaka, M. *Top. Curr. Chem.* **2004**, *232*, 25–54. (c) Glueck, D. S. in *Topics in Organometallic Chemistry*, Vol. 31: C–X Bond Formation (Ed.: A. Vigalok), Springer-Verlag, Berlin, Heidelberg, **2010**, pp. 65-100. (d) S. A. Pullarkat, P. H. Leung in *Topics in Organometallic Chemistry*, Vol. 43: Hydrofunctionalization (Eds.: V. P. Ananikov, M. Tanaka) Springer-Verlag, Berlin, Heidelberg, **2013**, pp. 145-166. (e) Koshti, V.; Gaikwad, S.; Chikkali, S. H. *Coord. Chem. Rev.* **2014**, 265, 52-73. (f) Greenhalgh, M. D.; Jones, A. S.; Thomas, S. P. *ChemCatChem* **2015**, *7*, 190-222. (g) Rodriguez-Ruiz, V.; Carlino, R.; Bezzenine-Lafollee, S.; Gil, R.; Prim, D.; Schulz, E.; Hannedouche, J. *Dalton Trans.* **2015**, *44*, 12029-12059.

2 (a) Shulyupin, M. O.; Kazankova, M. A.; Beletskaya, I. P. *Org. Lett.* **2002**, *4*, 761-763. (b) Kazankova, M. A.; Shulyupin, M. O.; Borisenko, A. A.; Beletskaya, I. P. *Russ. J. Org. Chem.* **2002**, *38*, 1479-1484.

3 (a) Huang, Y. H.; Chew, R. J.; Li, Y. X.; Pullarkat, S. A.; Leung, P. H. *Org. Lett.* **2011**, *13*, 5862-5865. (b) Xu, C.; Kennard, G. J. H.; Hennersdorf, F.; Li, Y. X.; Pullarkat, S. A.; Leung, P. H. *Organometallics* **2012**, *31*, 3022-3026. (c) Huang, Y. H.; Pullarkat, S. A.;

Teong, S.; Chew, R. J.; Li, Y. X.; Leung, P. H. *Organometallics* **2012**, *31*, 4871-4875. (d) Huang, Y. H.; Pullarkat, S. A.; Li, Y. X.; Leung, P. H. *Inorg. Chem.* **2012**, *51*, 2533.

4 (a) Pringle, P. G.; Smith, M. B. *J. Chem. Soc., Chem. Commun.* **1990**, 1701-1702. (b) Wicht, D. K.; Kourkine, I. V.; Lew, B. M.; Nthenge, J. M.; Glueck, D. S. *J. Am. Chem. Soc.* **1997**, *119*, 5039-5040. (c) Wicht, D. K.; Kourkine, I. V.; Kovacik, I.; Glueck, D. S.; Concolino, T. E.; Yap, G. P. A.; Incarvito, C. D.; Rheingold, A. L. *Organometallics* **1999**, *18*, 5381-5394. (d) Kovacik, I.; Wicht, D. K.; Grewal, N. S.; Glueck, D. S.; Incarvito, C. D.; Guzei, I. A.; Rheingold, A. L. *Organometallics* **2000**, *19*, 950-953. (e) Scriban, C.; Kovacik, I.; Glueck, D. S. *Organometallics* **2005**, *24*, 4871-4874. (f) Scriban, C.; Glueck, D. S.; Zakharov, L. N.; Kassel, W. S.; DiPasquale, A. G.; Golen, J. A.; Rheingold, A. L. *Organometallics* **2006**, *25*, 5757-5767.

5 (a) Douglass, M. R.; Marks, T. J. *J. Am. Chem. Soc.* **2000**, 1*22*, 1824-1825. (b) Douglass, M. R.; Stern, C. L.; Marks, T. J. *J. Am. Chem. Soc.* **2001**, *123*, 10221-10238. (c) Douglass, M. R.; Ogasawara, M.; Hong, S.; Metz, M. V.; Marks, T. J. *Organometallics* **2002**, *21*, 283-292. (d) Motta, A.; Fragala, I. L.; Marks, T. J. *Organometallics* **2005**, *24*, 4995-5003.

6 (a) Delacroix, O.; Gaumont, A. C. *Curr. Org. Chem.* **2005**, *9*, 1851-1882. (b) Chianese, A. R.; Lee, S. J.; Gagne, M. R. *Angew. Chem. Int. Ed.* **2007**, *46*, 4042-4059. (c) Glueck, D. S. *Chem. Eur. J.* **2008**, *14*, 7108-7117. (d) Glueck, D. S. *Top. Organomet Chem.* **2010**, *31*, 65-100. (e) Rosenberg, L. *ACS Catal.* **2013**, *3*, 2845-2855. (f) Koshti, V.; Gaikwad, S.; Chikkali, S. H. *Coord. Chem. Rev.* **2014**, *265*, 52-73.

7 (a) Leyva-Perez, A.; Vidal-Moya, J. A.; Cabrero-Antonino, J. R.; Al-Deyab, S. S.; Al-Resayes, S. I.; Corma, A. *J. Organomet. Chem.* **2011**, *696*, 362-367. (b) Isley, N. A.; Linstadt, R. T. H.; Slack, E.D.; Lipshutz, B. H. *Dalton Trans.* **2014**, *43*, 13196-13200.

8 (a) Erickson, K. A.; Dixon, L. S. H.; Wright, D. S.; Waterman, R., *Inorg. Chim. Acta* **2014**, *422*, 141-145. (b) Stelmach, J. P. W.; Bange, C. A.; Waterman, R. *Dalton Trans.* **2016**, DOI: 10.1039/C5DT04272K.

9 (a) Perrier, A.; Comte, V.; Moise, C.; Le Gendre, P., *Chem. Eur. J.* **2010**, *16*, 64-67. (b) Ghebreab, M. B.; Bange, Ch. A.; Waterman, R. *J. Am. Chem. Soc.* **2014**, *136*, 9240-9243. (c) Bange, C. A.; Ghebreab, M. B.; Ficks, A.; Mucha, N. T.; Higham, L.; Waterman, R. *Dalton Trans.* **2016**, *45*, 1863-1867.

10 (a) Crimmin, M. R.; Barrett, A. G. M.; Hill, M. S.; Hitchcock, P. B.; Procopiou, P. A. *Organometallics* **2007**, *26*, 2953-2956. (b) Liu, B.; Roisnel, T.; Carpentier, J.-F.; Sarazin, Y. *Angew. Chem. Int. Ed.* **2012**, *51*, 4943-4946. (c) Hu, H.; Cui, C. *Organometallics* **2012**, *31*, 1208-1211. (d) Liu, B.; Roisnel, T.; Carpentier, J.-F.; Sarazin, Y. *Chem. Eur. J.* **2013**, *19*, 13445-13462.

11 (a) Basalov, I. V.; Roşca, S.-C.; Lyubov, D. M.; Selikhov, A. N.; Fukin, G. K.; Sarazin, Y.; Carpentier, J.-F.; Trifonov, A. A. *Inorg. Chem.* **2014**, *53*, 1654-1661. (b) Basalov, I. V.; Dorcet, V.; Fukin, G. K.; Carpentier, J.-F.; Sarazin, Y.; Trifonov, A. A. *Chem. Eur. J.* **2015**, *21*, 6033-6036. (c) Basalov, I. V.; Yurova, O. S.; Cherkasov, A. V.; Fukin, G. K.; Trifonov, A. A. *Inorg. Chem.* **2016**, *55*, 1236-1244.

12 Moquist, P.; Chen, G.-Q.; Mueck-Lichtenfeld, C.; Bussmann, K.; Daniliuc, C. G.; Kehr, G.; Erker, G. *Chem.Sci.* **2015**, *6*, 816-825.

13 (a) Hou, Z.; Wakatsuki, Y. *Coord. Chem. Rev.* **2002**, *231*, 1-22. (b) Gromada, J.; Carpentier, J.-F.; Mortreux, A. *Coord. Chem. Rev.* **2004**, *248*, 397-410.

14 (a) Jeske, G.; Lauke, H.; Mauermann, H.; Swepston,, P. N.; Schumann, H.; Marks, T. J. *J. Am. Chem. Soc.* **1985**, *107*, 8091-8103. (b) Jeske, G.; Schock, L. E.; Swepston, P. N.; Schumann, H.; Marks, T. J. *J. Am. Chem. Soc.* **1985**, *107*, 8103-8110.

15 Molander, G. A.; Romero, J. A. C. *Chem. Rev.* **2002**, *102*, 2161-2185.

16 For reviews, see: (a) Hultzsch, K. C. *Adv. Synth. Catal.* **2005**, *347*, 367-391. (b) Mìller, T. E.; Hultzsch, K. C.; Yus, M.; Foubelo, F.; Tada, M. *Chem. Rev.* **2008**, *108*, 3795-3892. (c) Hannedouche, J.; Schulz, E. *Chem. Eur. J.* **2013**, *19*, 4972-4985.

17 (a) Douglass, M. R.; Marks, T. J. *J. Am. Chem. Soc.* **2000**, *122*, 1824-1825. (b) Douglass, M. R.; Stern, C. L.; Marks, T. J. *J. Am. Chem. Soc.* **2001**, *123*, 10221-10238. (c) Kawaoka, A. M.; Douglass, M. R.; Marks, T. J. *Organometallics* **2003**, *22*, 4630-4632. (d) Kawaoka, A. M.; Marks, T. J. *J. Am. Chem. Soc.* **2004**, *126*, 12764-12765. (e) Kawaoka, A. M.; Marks, T. J. *J. Am. Chem. Soc.* **2005**, *127*, 6311-6324. (f) Motta, A.; Fragala, I. L.; Marks, T. J. *Organometallics* **2005**, *24*, 4995-5003.

18 Weiss, C. J.; Marks, T. J. *Dalton Trans.* **2010**, *39*, 6576-6588.

19 (a) Harrison, K. N.; Marks, T. J. *J. Am. Chem. Soc.* **1992**, *114*, 9220-9221. (b) Bijpost, E. A.; Duchateau, R.; Teuben, J. H. *J. Mol. Catal. A* **1995**, *95*, 121-128.

20 Labouille, S.; Clavaguéra, C.; Nief, F. *Organometallics* **2013**, *32*, 1265-1271.

21 (a) Izod, K.; Clegg, W.; Liddle, S. T. *Organometallics* **2000**, *19*, 3640-3643. (b) Fedushkin, I. L.; Petrovskaya, T. V.; Bochkarev, M. N.; Dechert, S.; Schumann, H. *Angew. Chem. Int. Ed.* **2001**, *40*, 2474-2477. (c) Weber, F.; Sitzmann, H.; Schultz, M.; Sofield, C. D.; Andersen, R. A. *Organometallics* **2002**, *21*, 3139-3146. (d) Panda, T. K.; Zulys, A.; Gamer, M. T.; Roesky, P. W. *J. Organomet. Chem.* **2005**, *690*, 5078-5089. (e) Ruspic, C.; Spielmann, J.; Harder, S. *Inorg. Chem.* **2007**, *46*, 5320-5326. (f) Datta, S.; Gamer, M. T.; Roesky, P. W. *Organometallics* **2008**, *27*, 1207-1213.

22 Harder, S. *Angew. Chem. Int. Ed.* **2004**, *43*, 2714-2718.

23 Liu, B.; Carpentier, J.-F.; Sarazin, Y. *Chem. Eur. J.* **2012**, *18*, 13259-13264.

24 (a) Poirier, V.; Roisnel, T.; Carpentier, J.-F.; Sarazin, Y. *Dalton Trans.* **2009**, 9820-9827. (b) Sarazin, Y.; Liu, B.; Roisnel, T.; Maron, L.; Carpentier, J.-F. *J. Am. Chem. Soc.* **2011**, *133*, 9069-9087.

25 (a) Sockwell, S. C.; Hanusa, T. P.; Huffman, J. C. *J. Am. Chem. Soc.* **1992**, *114*, 3393-3399. (b) Crimmin, M. R.; Barrett, A. G. M.; Hill, M. S.; MacDougall, D.; Mahon, M. F.; Procopiou, P. A. *Dalton Trans.* **2009**, 9715-9717. (c) Arrowsmith, M.; Hill, M. S.; Kociok-Köhn, G. *Organometallics* **2011**, *30*, 1291-1294.

26 (a) Harder, S.; Feil, F.; Knoll, K. *Angew. Chem., Int. Ed.* **2001**, *40*, 4261-4264. (b) Piesik, D. F.-J.; Häbe, K.; Harder, S. *Eur. J. Inorg. Chem.* **2007**, 5652-5661. (c) Harder, S.; Feil, F. *Organometallics* **2002**, *21*, 2268-2274.

27 Liu, B.; Roisnel, T.; Guégan, J.-P.; Carpentier, J.-F.; Sarazin, Y. *Chem. Eur. J.* **2012**, *18*, 6289-6301.

28 Crimmin, M. R.; Barrett, A. G. M.; Hill, M. S.; MacDougall, D. J.; Mahon, M. F.; Procopiou, P. A. *Chem. Eur. J.* **2008**, *14*, 11292-11295.

29 Cloke, F. G. N.; Hitchcock, P. B.; Lappert, M. F.; Lawless, G. A.; Royo, B. *J. Chem. Soc., Chem. Commun.* **1991**, 724-726.

30 We have checked that the metal precatalysts were required to observe substrate conversion. The simple heating of $PhPH_2$ with one equivalent of styrene at 60 °C for 24h in C_6D_6 only resulted in 3% conversion towards the monoaddition product as a result of thermally induced homolytic cleavage of the P–H bond and 1,2-addition across the unsaturated bond. With two equivalents of styrene under otherwise identical conditions, 3% formation of the monoaddition product was again detected, with no detectable sign of formation of the double addition product.

31 Arrowsmith, M.; Crimmin, M. R.; Barrett, A. G. M.; Hill, M. S.; Kociok-Köhn, G.; Procopiou, P. A. *Organometallics* **2011**, *30*, 1493-1506.

32 Brinkmann, C.; Barrett, A. G. M.; Hill, M. S.; Procopiou, P. A.; Reid, S. *Organometallics* **2012**, *31*, 7287-7297.

33 X. Han, R. Lee, T. Chen, J. Luo, Y. Lu, K.-W. Huang, *Sci. Rep.* **2013**, *3*, 2557-2562.

34 Prikhod′ko, A. I.; Sauvage, J.-P. *J. Am. Chem. Soc.* **2009**, *131*, 6794-6807.

35 For the values of Hammett σ constants, see: Hansch, C.; Leo, A.; Taft, R. W. *Chem. Rev.* **1991**, *91*, 165-195.

36 The hypothesis of partial, gradual decomposition of the catalyst in the presence of the fluorinated substrate, as observed with *p*-CF_3-styrene, can be in principle ruled out considering the regular (linear) kinetic profile.

37 Atkins, P. W. Physical Chemistry, 5th ed.; Oxford University Press, **1994**.

38 Liu, B.; Roisnel, T.; Carpentier, J.-F.; Sarazin, Y. *Chem. Eur. J.* **2013**, *19*, 2784-2802.

39 (a) Girard, P.; Namy, J. L.; Kagan, H. B. *J. Am. Chem. Soc.* **1980**, *102*, 2693-2698. (b) Evans, W. J.; Drummond, D. K.; Zhang, H.; Atwood, J. L. *Inorg. Chem.* **1988**, *27*, 575-579.

40 (a) Sheldrick, G. M. SHELXS-97, Program for the Determination of Crystal Structures; University of Goettingen: Germany, **1997**. (b) Sheldrick, G. M. SHELXL-97, Program for the Refinement of Crystal Structures; University of Göttingen: Germany, **1997**.

41 Sheldrick, G. M. SHELXTL v.6.12, Structure Determination Software Suite; Bruker: Madison, WI, **2000**.

42 SCALE3 ABSPACK: Empirical absorption correction, CrysAlis Pro - Software Package, Agilent Technologies, **2012**.